Dalton Transactions

Accepted Manuscript

This is an *Accepted Manuscript*, which has been through the Royal Society of Chemistry peer review process and has been accepted for publication.

Accepted Manuscripts are published online shortly after acceptance, before technical editing, formatting and proof reading. Using this free service, authors can make their results available to the community, in citable form, before we publish the edited article. We will replace this *Accepted Manuscript* with the edited and formatted *Advance Article* as soon as it is available.

You can find more information about *Accepted Manuscripts* in the Information for Authors.

Please note that technical editing may introduce minor changes to the text and/or graphics, which may alter content. The journal's standard Terms & Conditions and the Ethical guidelines still apply. In no event shall the Royal Society of Chemistry be held responsible for any errors or omissions in this *Accepted Manuscript* or any consequences arising from the use of any information it contains.

ROYAL SOCIETY OF CHEMISTRY

www.rsc.org/dalton

Please do not adjust margins

Journal Name

Perspective

Metal-Ligand Cooperation at Tethered π-Ligands

Dide G. A. Verhoeven[a] and Marc-Etienne Moret*[a]

Received 00th January 20xx,
Accepted 00th January 20xx

DOI: 10.1039/x0xx00000x

www.rsc.org/

Metal-ligand cooperativity in homogeneous catalysis is emerging as a powerful tool for the design of efficient transition-metal catalysts. This perspective highlights recent advances in the use of neutral π-coordinating ligands, tethered to a transition-metal center by other donor ligands, as cooperative reaction centers. The state-of-the-art organometallic complexes, including π-coordinating ligands originating from C=C, C=E (E = O, N) and boron containing moieties, are described here, with special attention on their specific reactivity. Geometric and electronic aspects of ligand design and their influence on the coordination mode and reactivity of the π-system are discussed.

1 Introduction

Metal-ligand cooperativity is a fertile area of investigation for the development of modern homogeneous catalysts.[1, 2] Cooperative ancillary ligands do not only stabilize and tune the coordination environment of a metal center, but also engage in chemical reactions with substrate molecules, opening new reactive pathways. In particular, they are proving useful in controlling the reactivity of base metals in view of substituting widely used precious metals catalysts.[2, 3]

Metal-ligand cooperativity can take a number of forms. First, perhaps the simplest of those is hemilability,[4, 5] i.e. reversible dissociation of a electron donor (or acceptor) moiety that allows the coordination environment of the metal to adapt to the steric and electronic requirements of different reaction intermediates along a reaction mechanism. Then, redox-active ligands,[3] which act as electron reservoirs during catalysis due to the presence of low lying empty orbitals and/or high-lying filled orbitals at energies comparable to that of the metal *d* orbitals. This property has been used to facilitate multi-electron processes at metals that tend to undergo one-electron processes or even at redox inactive metals, maintaining the metals oxidation state throughout the process (Fig. 1).[1, 7-10] Finally, the category of bifunctional ligands broadly encompasses ligands that engage in bond-forming and bond-breaking events, working together with the metal in substrate activation *via* functional groups positioned at the ligand. A prominent example of bifunctional ligands are tethered amido ligands (R_2N–M) as found in Noyori-type catalysts for transfer hydrogenation,[11] which can accept a proton to become amine ligands ($R_2N(H)$-->M). This allows dihydrogen to be split heterolytically, leaving a hydride ligand on the metal center, to be subsequently transferred to an unsaturated substrate. Similar mechanisms have been proposed for many of the most efficient catalysts for the hydrogenation of polar bonds, *via* bifunctional H_2 activation involving a variety of internal bases such as deprotonated acidic CH_2 groups[12-14] or a coordinated cyclopentadienone[15-20] ligand. Bifunctional substrate activation is of interest for performing bond-making and bond-breaking processes with non-precious metals. In particular, this design principle has recently been used in the development of highly efficient iron-based catalysts for the (de)hydrogenation of polar substrates.[14, 21-25]

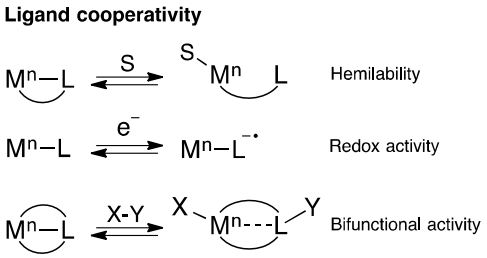

Figure 1. Ligand cooperativity in substrate activation.

The coordination of olefins and other π-ligands to transition metals is a staple of organometallic chemistry. Upon binding, electron density is transferred from the π-bonding orbital to the metal (σ-donation) and, concomitantly, d electrons are partially donated to the π-antibonding orbital. This reduces the bond order and activates the double bond towards both nucleophilic and electrophilic attack. As a result, several elementary steps are available to metal-bound olefins (Scheme 1): a) ligand exchange where an olefinic substrate binds to the metal *via* a vacant site, b) electrophilic or c) a nucleophilic attack while the olefin is already bound to the metal, or d) concerted processes such as β-insertion (Scheme 1). While these elementary steps are part of the mechanism of many catalytic transformations of unsaturated substrates, anchoring

[a] Organic Chemistry & Catalysis, Debye Institute for Nanomaterials Science, Utrecht University, Universiteitsweg 99, 3584 CG Utrecht, The Netherlands. Email: M.Moret@uu.nl

Dalton Transactions Accepted Manuscript

Please do not adjust margins

such motifs to a metal in a multidentate ligand represents an attractive design principle for cooperative ligand systems.

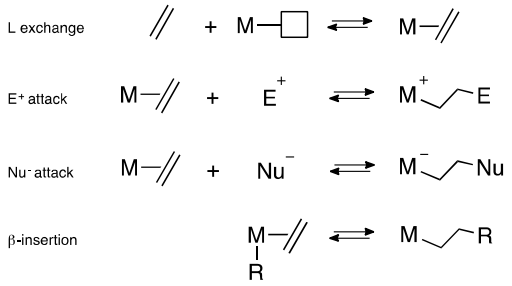

Scheme 1. Types of olefin activation on a metal center.

The relative lability of simple π-ligands requires them to be tethered *via* the ligand backbone, so that dissociation of the ligand will not occur. A stable and robust option are the tridentate pincer type ligands,[26-37] which gained much attention as robust redox-active or bifunctional ligands. Paralleling the elementary steps outlined in Scheme 1, anchored π-ligands may display a range of cooperative processes. Weakly bound ligands may display hemilability and adaptive coordination. Upon binding of a substrate, the multiple bond can accept either an electrophilic or a nucleophilic fragment, proton (H^+) and hydride (H^-) being prototypical examples. Hence, a small molecule X–Y can split in a heterolytic fashion, adding part of the substrate to the metal center and part to the ligand backbone, and so performing a two-electron bond-breaking process, split over both the ligand and the metal (Fig. 1).

This perspective highlights recent advances in the use of π-coordinating ligands in the design of cooperative ligands. First, pincer ligands incorporating π-coordinating C=C moieties, including aromatic systems, are discussed in Section 2. Systems containing an activating borane moiety conjugated with a carbon-based π-system are covered in Section 3. Finally, π-interactions of C=E bonds (E = O, NR) are described, including carboxyl and imine based systems (Chapter 4).

2 π-coordinating C=C bonds

2.1 Olefin complexes

A first class of ligands that can be envisioned to act as cooperative ligands in catalysis are olefins. This well known class of ligands has been studied in detail, starting from the first organometallic complex ever reported, i.e. Zeise's salt ($K[PtCl_3(C_2H_4)]\cdot H_2O$).[38] A metal can bind to an olefinic C=C bond *via* its d_σ orbital to the ligands π-electrons, forming the σ-bond. Next to this, the metal d_π orbitals can donate electrons to the LUMO of the ligand, the C=C π*, *via* π-backdonation. Lengthening of the olefinic C=C bond is obtained to which both factors contribute, but the latter effect predominates. The resonance structures that can be drawn for these interactions, shown in Fig. 2a, follow the Dewar-Chatt-Duncanson model; the side-on bound adduct which gives a L type ligand and the metallacyclopropane adduct which gives a X_2 type ligand.[7] The difference in the binding mode causes a change in the oxidation state of the metal center, i.e. the metal oxidation state remains the same in the L-type bound ligand and it increases by two in the X_2-type binding, causing ambiguity in the oxidation state of the metal. Throughout this perspective we will generally refer to the lower oxidation state.

Strong bonds are formed with electron rich metal centers, as backdonation will be most efficient.[39] This bond can be formed or broken depending on the metal oxidation state, possibly functioning as a hemilabile ligand and directing the system toward bifunctional behavior. One way of activating a small molecule X–Y on such systems is *via* changing the ligands coordination mode, forming a σ-bond with one of the olefinic carbons and adding X to the metal center, together with addition of Y to the second olefinic carbon (Fig. 2b). Internal alkenes and alkynes are classes of ligands that have shown to be suitable as π-coordinating ligands.

Figure 2. a) Resonance extremes of an alkene binding to a metal center, left: side-on adduct, right: metallacyclopropane adduct. b) Addition of a substrate X-Y to this bond, altering the binding mode to form a σ-bond with one of the olefinic carbons.

The use of phosphine-substituted *trans*-stilbenes as π-coordinating ligands was investigated in detail by several groups. The *ortho*-diphosphine *trans*-stilbene ligand *t*PCH=CHP contains two phosphorus groups to bind the metal center in a bidentate fashion bridged via the olefinic ligand backbone which can coordinate to the metal center in a η^2-fashion (Fig 3). The incorporation of this ligand in metal complexes was first described by the group of Bennett in 1976.[40] The complexation to rhodium and iridium was described, in which the desired η^2-coordination of the olefinic backbone was indeed observed, as was shown by NMR analysis and the elongation of the C–C bond in X-ray crystal structure analysis of the ^{o}Tol-Rh-Cl complex. The coordination to group 10 metals Ni, Pd and Pt in the oxidation state of two was shown to result in a different coordination mode, in which a σ-bond was formed with one of the olefinic carbon atoms under elimination of HX.[39]

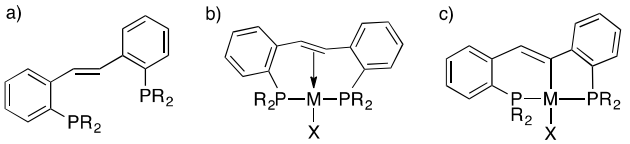

Figure 3. From left to right: a) trans-stilbene-type ligand: *t*PCH=CHP, R = *o*-Tol or Ph; b) η^2 coordination complexes M = Rh, Ir, R = Ph, X = Cl, Br, I; c) σ-coordination complexes M = Ni, Pd, Pt, R = ph, *o*-Tol, X = Cl.

The Rh and Ir complexes were shown to bind CO and subsequently cleave HCl in a heterolytic fashion over the metal –olefin fragment. This results in the addition of chloride to the metal center and a proton to the ligand backbone, inducing the formation of a C–M σ-bond with one of the olefinic carbon atoms (Scheme 2).[40] The reaction can formally be seen as a

This journal is © The Royal Society of Chemistry 20xx

Dalton Transactions Accepted Manuscript

Please do not adjust margins

electrophilic attack of H^+ at the olefin (Scheme 1). It shows an early example of cooperative behavior of the olefin ligand with the metal center.

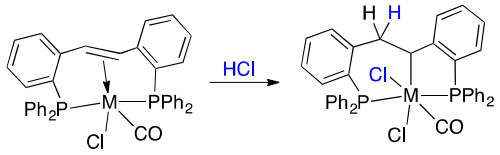

Scheme 2. σ-complexes after addition of CO and subsequent cooperative addition of HCl, M = Rh, Ir.

A different approach for making a similar ligand was reported by Baratta *et al*. Here, the carbon-carbon double bond was formed from two *o*-methyl groups of two phosphines, as a result of activation of four C–H bonds, leaving an *ortho*-tolyl substituted *trans*-stilbene-type ligand, $^{o\text{Tol}}$*t*PCH=CHP (Scheme 3). An osmium(II) complex was synthesized of which the X-ray crystal structure showed an elongation of the C=C bond (1.437(4) Å), as a result of η^2-coordination to Os.[42]

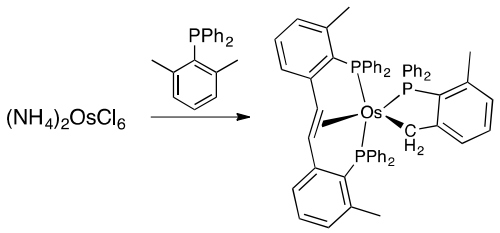

Scheme 3. Synthesis of an Os(I) complex of the $^{o\text{Tol}}$*t*PCH=CHP ligand from 2,6-xylylPPh$_2$ and $(NH_4)_2OsCl_6$ upon activation of four C-H bonds.[42]

The use of the *t*PCH=CHP ligand was extended in the group of Iluc, with the aim of using its backbone as an hydrogen atom reservoir, i.e. noncoordination and η^2-coordination in the neutral form and η^1-coordination in the vinyl form which could store hydrogen.[43] After modification of the ligand by incorporating di-*iso*-propylphenyl ligands, σ-coordination metal complexes were synthesized with Ni, Pd and Pt resulting from C–H activation of the backbone, followed by rapid reductive elimination of HCl. Interestingly, H transfer was observed for the nickel analogue **(*t*PC=CHP)NiCl** upon addition of Li[Et_3BH], first forming a hydride ligand on the metal center which was then transferred to the backbone resulting in a Ni(0) complex **(*t*PCH=CHP)Ni** with η^2-binding of the olefin (Scheme 4).

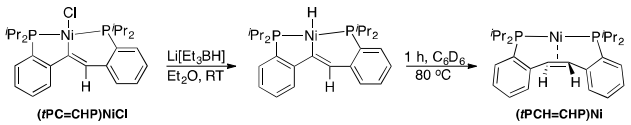

Scheme 4. The **(*t*PC=CHP)NiCl** complex and the observed H-transfer upon addition of Li[Et_3BH] to **(*t*PCH=CHP)Ni**.

η^2-Coordination of the ligand was also established for nickel(II), upon substitution of the olefinic protons for methyl groups, eliminating the possibility of HCl loss. 2 eq of *t*PCMe=CMeP were mixed with 3 eq of $NiCl_2$(dme), resulting in a cationic mono chloride species with a $NiCl_4^{2-}$ counteranion, **[(*t*PCMe=CMeP)NiCl]$_2$[NiCl$_4$]**. The complex displays a square-planar geometry around the Ni(II) center and an elongated C–C bond distance for the olefinic backbone (1.398(3) Å vs 1.330(4) Å).

Synthesis of the more electron-rich analogues Ni(I) *t*PCH=CHP complex, without a counterion, was performed next by a comproportionation reaction using the nickel(II) and nickel(0) precursors $NiCl_2$(dme) and $Ni(cod)_2$ (Chart 1). Analysis by single crystal X-ray spectroscopy showed a tetrahedral geometry around the nickel(I) center and an olefinic C–C bond distance of 1.394(3) Å indicative of a η^2-interaction, without the need to incorporate methyl groups on the ligand backbone. η^2-Coordination was also observed for the previously described Ni(0) complex **(*t*PCH=CHP)Ni**, now directly synthesized from the ligand and $Ni(cod)_2$, which showed activity upon addition of 1 eq MeI, forming a cationic methyl nickel complex, **[(*t*PCH=CHP)NiMe]I** (Scheme 5).[43]

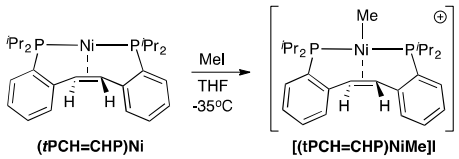

Scheme 5. Reaction of the η^2-coordinated Ni(0) complex **(PCH=CHP)Ni** with MeI resulting in **[(*t*PCH=CHP)NiMe]I**.

The hemilability of this system was shown with the Fe and Co analogues.[44] The Fe(II) and Co(II) complexes (*t*PCH=CHP)MX_2 were synthesized, both containing a non-coordinated olefin moiety, with distances from the metal center to the ligand centroid of 3.596 Å for L$FeBr_2$ and 3.501 Å for L$CoCl_2$ (Chart 1). A weak interaction was obtained after halide abstraction of both complexes with Na[$BAr^F{}_4$], shown by the slight elongation of the olefinic C–C ligand backbone (ligand: 1.330(4) Å; Fe: 1.332(14) Å; Co: 1.397(6) Å, Chart 1). A strong interaction was obtained after synthesis of the analogous neutral Co(I) complex **(*t*PCH=CHP)MCl** by reduction of the Co(II) complex with $LiAlH_4$ (Chart 1). The ^{1}H NMR spectrum shows a significant upfield shift for the olefinic protons to 2.01 ppm (for *t*PCH=CHP at 8.53 ppm), which is consistent with a bound olefinic moiety with significant π-backdonation. The bond distances were found to be in line with this observation, as an elongation was found for the C–C backbone from 1.397(6) Å in the unbound Co(II) complex to 1.442(5) Å in the bound Co(I) complex. The higher degree of backbonding was attributed to the more electron rich Co(I) system compared to the cationic Co(II) species. A similar system was found for the square-planar rhodium analogue **(*t*PCH=CHP)RhCl**, in which significant π-backdonation of the bound olefin was shown by upfield shifted olefin protons and an elongated C–C distance of 1.432(8) Å (Chart 1). Group 11 metals were explored by the synthesis of the Cu and Ag analogues. Bonding of the olefin was in both cases not observed, although a weak interaction could not be excluded for the Cu(I) complex **(*t*PCH=CHP)Cu(OTf)**: a relatively short distance between the metal and the ligand centroid was observed (2.426 Å), but the olefinic C=C bond lacked elongation (1.294(5) Å). Also the

Dalton Transactions Accepted Manuscript

Please do not adjust margins

synthesis of cationic divalent complexes, without a halide or triflate ligand, did not lead to interaction with the backbone but afforded linear complexes.[44]

Overall it was observed that the olefinic C=C bond of *t*PCH=CHP elongates upon coordination to a metallic center, predominantly upon binding to an electron rich metal. Bond lengths ranging from 1.40 to 1.44 Å were observed for olefin bound metal complexes, of which the longest C=C length of 1.442(5) Å was observed for **(*t*PCH=CHP)CoCl**, showing efficient coordination to the electron rich cobalt center. A large upfield shift in both ^{1}H and ^{13}C NMR was observed in all cases for coordination of the olefin backbone, showing the increased electron density on the ligand backbone. *t*PCH=CHP is a promising ligand for the activation of small molecules as it is observed to bind to numerous metal centers and the ligand binding mode shows great versatility.

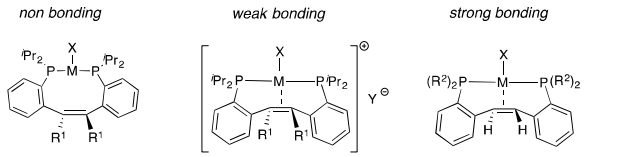

Chart 1. Overview of the non-bonding and η^2-bonding trans-stilbene complexes, arranged by their binding mode.

In a separate study in the group of Iluc toward radical trapping, a Pd complex was obtained with a η^2-coordinating olefinic moiety in the backbone of the ligand. This complex was synthesized, among others, from a Pd-PCP pincer complex that reacted with CH_2X_2 to obtain **Pd-B** after CH_2 transfer to the coordinated nucleophilic carbon atom (Scheme 6). This novel type of CH_2 transfer was characterized by X-ray crystal structure analysis, next to other techniques, after direct synthesis of the complex, in which the elongation of the C–C bond was observed probably due to π-backbonding (1.398(3) Å vs. 1.34 Å for a C(sp^2)– C(sp^2)).[45] Complex **Pd-B** could also be independently synthesized by dehydrogenation of the corresponding saturated diphosphine ligand upon coordination to Pd. The 1,1-disubstitution pattern found in this ligand, contrasting with the 1,2-disubstitution pattern in the trans-stilbene derivatives, may open up distinct reactive pathways and certainly warrants further investigation.

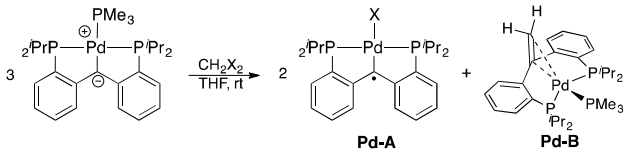

Scheme 6. Reaction of the Pd-PCP pincer complex with CH_2X_2 to form the expected halide complex **Pd-A** and unexpected CH_2 transfer product **Pd-B**.

An iridium-based system in which an internal olefin connected to a cyclohexyl ring binds in a η^2-fashion was synthesized in the group of Wendt (Scheme 7). The olefin binds in a similar fashion as was found for **Pd-B**, but having both carbon atoms bound to the ligand. The complex was formed from a PCP-pincer complex with a cyclohexyl backbone bound to Ir(III) with a phenyl and a hydride co-ligand. Upon heating in the presence of *tert*-butylethylene as a hydrogen acceptor, the α-carbon of one of the methyl groups of the *t*-butyl substituent was coupled to the Ir-bound carbon atom to form a new coordinated olefin functionality, **IrPh**. This bond-making process was found to be reversible under an H_2 atmosphere at 140 °C.[46] The formed Ir(I) complex has a distorted square-planar geometry around the metal center, average Ir–C bond lengths of 2.16 and 2.20 Å and a C=C bond length of 1.42 Å, which are all in line with other electron rich Ir-olefin complexes[47] and the before mentioned distances for the elongation of the olefin backbone.

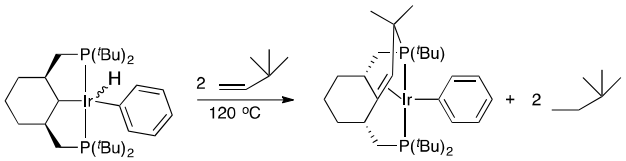

Scheme 7. The iridium based PCP-pincer complex and its subsequent reaction toward the η^2-bound complex.

The olefinic iridium complex was found to be active (Fig. 4) toward the addition of O_2, performing an oxidative addition over Ir cleaving the Ir–Ph bond (**IrO_2**), to $CHCl_3$ by replacing the phenyl ligand for a chloride (**IrCl**), and to CO by addition of a CO molecule to the metal center (**IrCO**). The product of the last reaction was shown to react with trifluoroacetic acid in an interesting way. First the Ir(I)-bound olefinic moiety was protonated, resulting in the unstable Ir(III) alkyl complex **$IrOCOCF_3$-*I***. A similar type of protonation of the backbone was shown before in the example of Bennett with the *trans*-stilbene-type ligands where addition of HCl lead to protonation of the backbone and the addition of Cl to the metal center (*vide supra*). **$IrOCOCF_3$-*I*** reacted further cleaving both the phenyl and CO bonds with iridium, forming benzaldehyde together with the proton and forming a bond between Ir and the trifluoroacetate anion (**$IrOCOCF_3$**).[48] Further reactivity of **IrPh** was explored with CO_2 and N_2, but no reaction was observed.[48] Exposure to H_2 showed the formation of hydride complexes that are in equilibrium, i.e. an olefinic complex with three hydride ligands on Ir and a PCP-pincer complex that added another H_2 molecule, split over the metal center and the ligand backbone **IrH**. This addition constitutes an interesting example of cooperative H_2 activation over a metal-olefin reactive center.[46]

Dalton Transactions Accepted Manuscript

This journal is © The Royal Society of Chemistry 20xx

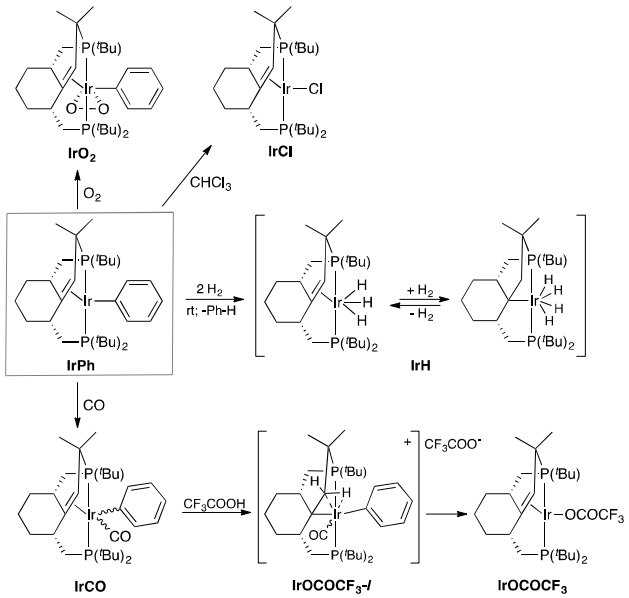

Figure 4. Reactivity study of the η^2-bound iridium complex with O_2, $CHCl_3$, H_2, and CO with the subsequent reaction of CF_3COOH.

Recently, a related PCP-Ir based complex with a terminal olefin was synthesized. Starting from the ligand with a methyl substituted cyclohexyl-group, an equilibrium was observed between an agostic η^2 C–C bond and the non-agostic structure (Fig. 5). Heating of the complex to 80 °C lead to the formation of H_2 via β-elimination, and a η^2-interaction with the olefin. Analysis by X-ray crystallography showed a C=C distance of 1.438(15) Å, which is in line with previously described η^2-bound complexes.[49]

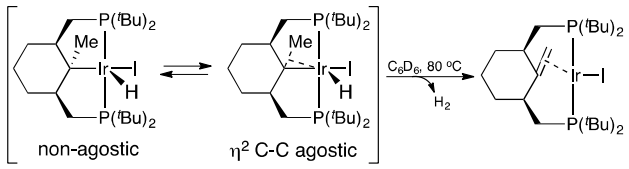

Figure 5. PCP-Ir complex and its reaction to the η^2-bound complex.

Besides the previously described systems based on a diphosphine/olefin architecture, related ligands have recently been studied using sulfur as the anchoring ligands, or an alkyne as the π-coordinating ligand.

A family of complexes containing an internal alkene moiety in a thione based ligand was developed in the groups of Han and Jin (SCCS, Fig. 6a).[50] The metallic center, Ir, Rh or Pd, was bound to the ligand in a bidentate fashion *via* the sulfur atoms and a coordination of the olefinic part was established either directly or after halide abstraction (Fig. 6b,c). The carbon-carbon double bond was found to elongate from 1.325(5) Å to 1.411(5) upon interaction with the metal center in **[(meSCCS)Ir(Cp*)]2Cl** (M = Ir, X = Cl, R = Me, Fig. 6b and Fig. 7, C(5)–C(6)).

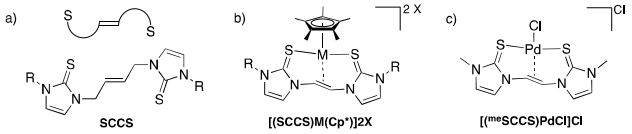

Figure 6. a) Schematic (top) and chemical structure (bottom) of SCCS. R = Me, $CH=CH_2$. b) General structure of the Ir and Rh complexes. M = Ir, X = Cl, R = Me, $CH=CH_2$; M = Ir, X = OTf, NO_3, R = Me; M = Rh, X = OTf, R = Me, $CH=CH_2$. c) Structure of the Pd complex.

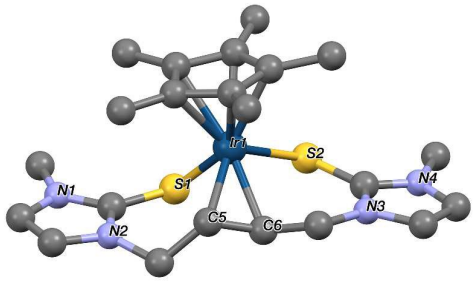

Figure 7. X-ray crystal structure of **[(meSCCS)Ir(Cp*)]2Cl**.[50]

The coordination of an alkyne ligand can be envisioned in a similar way, via π-coordination of the triple bond to the metal center. Such a system was explored by Ohe *et al.* using *ortho*-diphenylphosphinodiphenylacetylene (PCCP) as the ligand. This ligand contains an internal alkyne moiety connected to two phosphorus groups via phenyl rings (Fig. 8a).[51] The reaction of PCCP with an equimolar amount of $[RhCl(cod)]_2$ (cod = 1,5-cyclooctadiene) resulted in the η^2-alkyne-rhodium(I) complex **Rh(PCCP)Cl**, binding PCCP in a pincer-like multidentate fashion (L_3), and a chloride ligand (Fig. 8b). The Rh(I) complex adopts a square planar geometry in which the alkyne carbons lie parallel to the ML_3 plane. When the mixture of PCCP and rhodium precursor was heated for longer time and at higher temperatures (48 h, 50°C) a dimeric-rhodium species was synthesized **$[Rh(PCCP)Cl]_2$**, and X-ray crystallography showed the formation of a cyclobutadiene ligand generated by the dimerization of the chloride-complex. The cyclobutadiene ring was shown to have two η^2-coordinations to the rhodium atoms located on the opposite faces (Fig. 8b). Upon exchanging the chloride ligand of **Rh(PCCP)Cl** for CO, leaving a cationic complex after halide abstraction with $NaPF_6$ (**Rh(PCCP)CO**) backdonation from Rh to the alkyne ligand was weakened due to the stronger *trans* influence of CO, as shown in the X-ray crystal structure by longer Rh–C bond distances with the acetylenic carbons C(2)–C(3) compared to the chloride bound complex (2.203(7) and 2.199(6) for the Cl vs. 2.107(3) and 2.114(3) for the CO complex, Fig. 9).

Dalton Transactions Accepted Manuscript

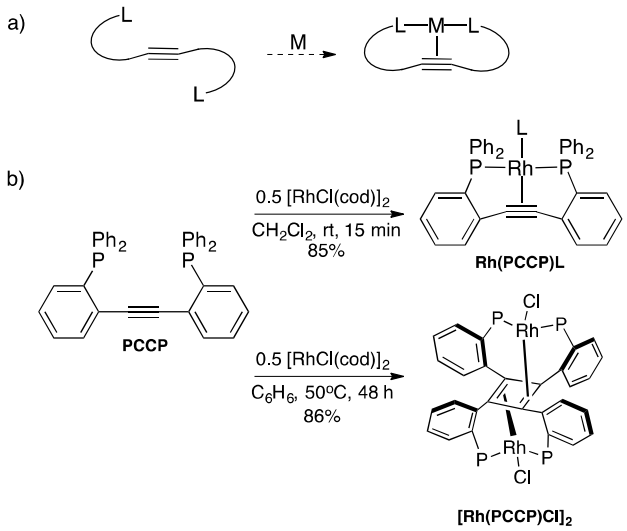

Figure 8. a) Schematic representation of the alkyne-M binding. b) The coordination of PCCP to Rh and the formation of a dimeric-Rh species, L = Cl or L = CO with PF_6^-; P = PPh_2. Figures adopted from Ohe et al.[51]

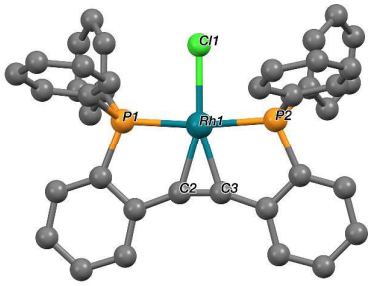

Figure 9. X-ray crystal structure of **Rh(PCCP)Cl**.[51]

Next to olefinic C=C bond coordination, π-coordinating arene groups are also of interest and are discussed next.

2.2 Aromatic complexes

Aromatic ligands containing a six-membered ring can bind to a metal center, forming a η^2, η^4 or η^6-bound complex. Interactions of an aromatic ring with a metal center are in general strong in comparison to hemilabile binding of olefin complexes, and η^6-arene ligands are often used as robust ancillary ligands. Cooperative activity can nevertheless be observed in such systems if the M–arene interaction is destabilized by strain in the ligand system and/or bulky substituents, or in the case of late transition metals which cannot easily accommodate a 6-electron donor in their valence shell. Heterolytic activation of a small molecule can occur in arene-based systems *via* splitting a molecule, X-Y, over the metal center and the aromatic ring, and so these systems are of interest to explore for their cooperative behavior.

Hemilabile arene coordination was used to prepare two-legged piano stool rhodium complexes that display unusual reversible electrochemical conversion between the oxidation states of I and II, using a 1,4-bis[4-(diphenylphosphino)butyl]-2,3,5,6-tetramethylbenzene (^{ph}PArP) ligand. The ligand was designed to have a long tether between the anchoring phosphine groups close to the metal center and the arene ring, in the form of the butyl chain, to accommodate flexibility of the ligand and its binding mode upon structural or electronic changes of the complex.[52] A Rh(I) complex was synthesized using ^{ph}PArP and $[Rh(THF)_2(COE)_2][PF_6]$, resulting in a complex with a rhodium center bound to two phosphorus atoms and an η^6-coordinated arene ring (Fig. 10a). The complex, **(^{ph}PArP)Rh(I)**, was chemically oxidized using $AgPF_6$, resulting in the dicationic Rh(II) analogue **(^{ph}PArP)Rh(II)** (Fig. 10a). The arene ring coordinates to the metal center in both oxidation states, but it was shown that the Rh(II) complex contains generally shorter Rh–C bond distances. **(^{ph}PArP)Rh(I)** showed reactivity toward small molecules, such as CO, acetonitrile and *tert*-butyl isocyanide, in a way that the interaction with the arene ligand was broken upon addition of other ligands (Fig. 10a).[53] A tricarbonyl species was formed upon exposure of the Rh(I) piano-stool complex to 1 atm CO, although reaction was slow and took over 20 days at room temperature.[53] Reactions with CO in acetonitrile resulted in binding of a CO and an acetonitrile molecule, and reaction with *tert*-butyl isocyanide resulted in binding of two of these ligands, again breaking the Rh–arene interaction in both cases. Similar reactivity was observed for the **(^{ph}PArP)Rh(II)** analogue with both CO and *tert*-butyl isocyanide, although reactions proceeded faster as explained by a generally higher reactivity of 17-electron complexes toward substitution reactions compared to their 18-electron counterparts (Fig. 10a). The Rh(II) complex was additionally reduced under a CO atmosphere or upon addition of *tert*-butyl isocyanide, forming the same complexes as obtained before by reaction of the Rh(I) analogue, **(^{ph}PArP)Rh(I)(CO)$_3$** and **(^{ph}PArP)Rh(I)L$_2$**, respectively. One of the key features to obtain this interaction was indeed found to be the tether length, as it needed to be long enough to accommodate structural changes upon complex oxidation. This shows that an arene-based system can contain hemilability in the sense of making and breaking the interaction with the ligand backbone when needed. The interaction between the metal center and the π-electron cloud is broken upon addition of substrates, resulting in vacant sites for these extra incoming ligands. In a next example of an envisioned M–arene interaction an *m*-terphenyl scaffold was used as the ligand (Fig. 10b). Here, no interaction with the explored metals was obtained as M–L distances of 3.51, 3.48 and 3.37 Å were obtained for the nickel, palladium[54] and rhodium[55] complexes, respectively. In this case the distance from the metal center to the closest arene–H is mentioned, due to its geometry. Nevertheless, for the rhodium complex containing the significantly shorter M–L distance, an interaction between the metal center and the π-electron cloud is observed as shown in the corresponding ^{1}H NMR spectrum where the aromatic protons of the central arene ring were distributed in a range of δ 6.18-8.04 ppm.[55]

Dalton Transactions Accepted Manuscript

This journal is © The Royal Society of Chemistry 20xx

Please do not adjust margins

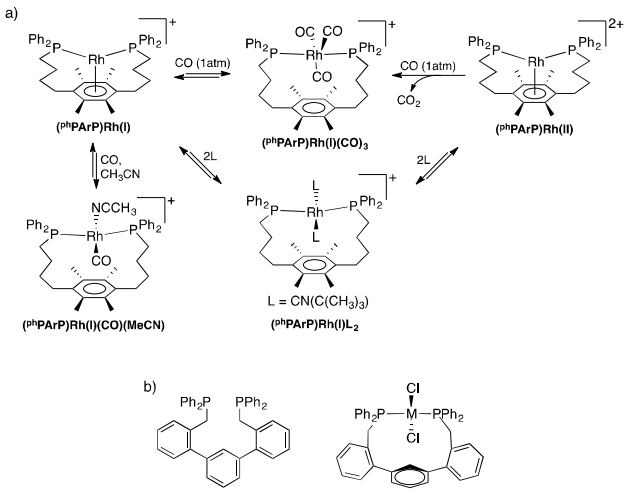

Figure 10. a) Two-legged piano stool based rhodium complexes and their reactivity. b) *m*-Terphenyl based ligand (left) and the corresponding divalent metal complexes (right) M = Ni, Pd or Rh.

Another strategy to obtain an Ar–M interaction is to keep the tether sufficiently short in combination with a flexible ligand backbone, so that the arene moiety is forced in close proximity to the metal center. The combination with a late transition metal (such as Ni(0)) that cannot readily accept 6 electrons from the aromatic ring results in enhanced reactivity. The use of a *p*-terphenyl diphenylphosphine (P_2terph, Fig. 12) ligand was designed and explored in the group of Agapie. The phosphorus groups are on the *ortho* positions of the two peripheral phenyl rings, creating a geometry with a short M–L distance upon coordination to a metal. Several systems with this ligand are explored,[56-59] but only selected cases are described here. In general, two ways of cooperative behavior are described, in which a) the ligand acts as an electron reservoir in combination with coordinative flexibility to stabilize different oxidation states, or b) the ligand backbone is activated and can form bonds with H-atoms or small molecules. A prominent recent example of the first case is a Mo-based complex, in which the *p*-terphenyl ligand stabilizes the formal oxidation states of Mo^{II}, Mo^{0}, Mo^{-II}, and Mo^{-III} (Fig. 11),[60] allowing for a remarkable deoxygenative reductive coupling of two metal-bound CO molecules. The redox active behavior of the tethered aromatic ring holds promise for catalytic reactions involving multi-electron transformations, such as the valorization of carbondioxide.

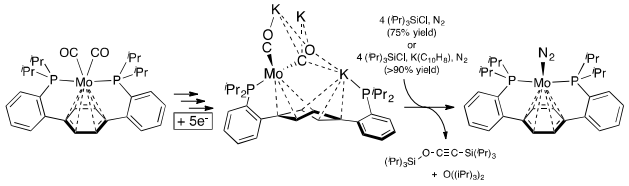

Figure 11. *p*-Terphenyl based Mo-complexes.

Chemical cooperativity at the aromatic ring was demonstrated with nickel-based systems. The solid state structure of a **Ni(0)(P_2terph)** complex, formed from a reaction of P_2terph with $Ni(cod)_2$, showed an interaction of the nickel center with both phosphines and a double bond of the arene backbone with Ni–C lengths of 1.992(1) and 2.002(1) Å. The chelation of the nickel center induced a bend of the peripheral aryl rings of 14° inwards relative to *p*-terphenyl.[61] The **Ni(0)(P_2terph)** complex was exposed to $Ni(II)Cl_2$(dme) to perform a comproportionation reaction, resulting in a dinuclear Ni^{I}–Ni^{I} complex **Ni_2(P_2terph)Cl_2**, coordinated *via* the phosphines in an almost linear PNiNiP fashion. To accommodate this binding, the peripheral aryl rings bent outwards with 16°. Furthermore, two bridging chloride ligands are bound to the nickel centers next to an arene–M interaction *via* two neighboring double bonds in the arene backbone.

Addition of HCl to **Ni(0)(P_2terph)** resulted in oxidative addition of the substrate to the nickel center and loss of the arene–nickel bond (Ni–C_{arene}: >2.5 Å) with only a weak interaction with the arene π-system.[62] Another dinuclear complex was formed upon heating of **Ni(P_2terph)HCl**, resulting in a **Ni_2(P_2terphH_2)Cl_2** with two bridging chloride ligands and the phosphorus ligands bound to the Ni(I) centers in a PNiNiP fashion, similar to the previously described dinuclear structure. The protons that were bound to nickel migrated to one of the double bonds of the aromatic rings, resulting in a single bond with a C_{ar}–C_{ar} distance of 1.5198(1) Å breaking the aromaticity. The Ni_2Cl_2 center interacts with the remaining four conjugated carbon atoms in the ring. To study the H-migration, a halide abstraction was performed starting from **Ni(P_2terph)HCl**, affording the positively charged **Ni(P_2terph)H** complex. Only a H was bound to the nickel center, which was stabilized by an η^2-interaction of the arene ring (Ni–C_{Ar}: 2.142(3) and 2.157(3) Å). Analysis by NMR and X-ray crystallography in combination with isotopic labeling experiments shows that the metal hydride can migrate to the aromatic ring, either to the *ipso* or *ortho* carbon (Fig. 12), demonstrating the possibilities of this system to store part of the substrate in the ligand backbone, which is a possible way of introducing cooperative behavior in the system.

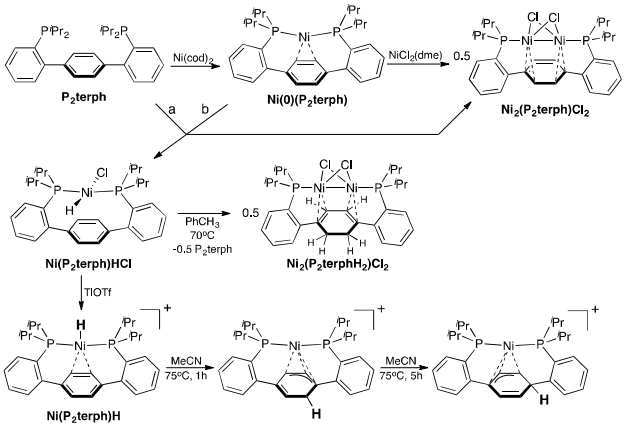

Figure 12. The p-terphenyl based ligand P_2terph and its coordination to nickel. a: $Ni(cod)_2$, $NiCl_2$(dme), b: HCl, Et_2O.

Besides the incorporation of a C-H based aromatic ring, the use of heteroatom containing rings is of interest. The incorporation of pyridine in the ligand backbone was investigated, binding the phosphorus tethers on the *meta*

Dalton Transactions Accepted Manuscript

Please do not adjust margins

positions, keeping a symmetrical ligand system. A diphosphine pyridine (PPyP) ligand was designed, in which the ligand can bind to the metallic center via its phosphorus atoms positioned on the ortho positions of the peripheral rings, as well as the heterocycle π system (Fig. 13).[63, 64] Nickel and palladium complexes were synthesized in which the aromaticity was disrupted due to an interaction with one of the carbon-carbon double bonds of the pyridine backbone. This was shown by a significant upfield shift in the ^{1}H NMR spectrum of **Ni(PPyP)** in which the central pyridine protons shifted, i.e. the *ortho*-pyridyl shifted to 7.82 ppm and the *para*-pyridyl protons to 4.35 ppm (respectively 8.96 ppm and 7.89 ppm in the free ligand), indicating a severe change in the electronic environment. Binding of a Lewis acidic group such as $B(C_6F_5)_3$ to the pyridine nitrogen atom enhanced the strength of this interaction between the ring and the metal center further, as was evident in further upfield shift of the *para*-pyridyl proton shifted to 3.18 ppm in **Ni(PPyBP)** (Fig. 13b). The electron-withdrawing $B(C_6F_5)_3$ group enhances the π-acceptor feature of the ligand, and so enhances the bond strength from the electron rich Ni^0 center to the π-system of the pyridine ligand. Activation of small molecules, such as HBpin, $PhSiH_3$ and $[Na][HBEt_3]$ was shown to take place in a stoichiometric fashion by breaking the aromaticity of the pyridine ring. In case of HBpin and $PhSiH_3$ the heteroatom binds to nitrogen and hydrogen to the carbon at the *ortho* position (Fig. 13c). In case of $[Na][HBEt_3]$ the activation took place on a methylated version of the nickel complex **Ni(PPyMeP)**, which was synthesized by addition of methyl triflate resulting in the methylated nitrogen atom and a triflate counter ion. Subsequent reaction with $[Na][HBEt_3]$ resulted in the breaking of the aromaticity by addition of a hydrogen atom to the carbon at the *ortho* position of nitrogen (Fig. 13d). This ligand-based reactivity was attributed to the metal-ligand bond, in which the pyridine aromaticity was disrupted resulting in a somewhat activated ligand backbone.[63]

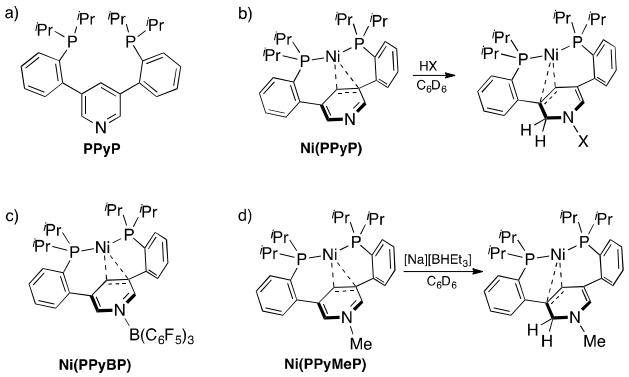

Figure 13. a) PPyP ligand. b) Ni(PPyP) and its activation of HX, HX = HBPin or H_3PhSi. c) The Ni(PPyBP) complex with $B(C_6F_5)_3$ bound to the nitrogen atom of the pyridine ring. d) Ni(PPyMeP) and its reaction with $[Na][BHEt_3]$.

3 π-Systems incorporating a boron atom

The last example showed how introducing an electronegative element in a conjugated π-systems can be used to increase its affinity for hydrides and enhance reactivity. A similar, maybe stronger, effect can also be achieved by conjugation with an electron deficient group such as a borane.

Boranes themselves can act as Z-type, σ-acceptor ligands that bind to a metal center via accepting an electron pair of the metal center, formally forming a retrodative bond.[65] They are often tethered to L-type ligands such as a phosphines for stabilization on the metal center, forming so called ambiphilic ligands.[66] Following the discovery of the first metallaboratrane by Hill in 1999,[67] ambiphilic ligands have attracted much interest because of their ability to stabilize unusual electronic structures and to act as cooperative ligands, as has been covered in several excellent reviews.[68-71] In many cases, the boron atom bears conjugated aromatic substituents that can also engage in binding to the metal, resulting in η^2(BC) or η^3(BCC) coordination modes. The chemistry of acylic boron-containing π-ligand complexes has been reviewed in 2012 by the group of Emslie.[72] Here we discuss selected recent examples highlighting the specific reactivity of this motif.

The use of ambiphilic phosphine-borane based ligands in Pd catalyzed Suzuki-Miyaura reactions was explored in the group of Bourissou.[73, 74] Boron-based ligands containing three aromatic substituents, of which one phosphorus-substituted, were synthesized (**PB1** and **PB2**, Fig. 14) and their activity as co-ligands was explored. The addition of **PB1** or **PB2** to a standard cross-coupling reaction with a Pd(II) precursor, such as $PdCl_2$(cod), Pd(ma)(nbd) or Pd_2dba_3, resulted in good yields for 2-chloropyridine, chloro-N-heterocycles and amino-2-chloropyridines. To better understand the effect of adding a Lewis acidic substituent in the form of a borane to this catalytic reaction, a closer look was taken at the *in situ* formed Pd-complexes. **Pd-PB1** was isolated in which an extra coordinated maleic acid ligand was coordinated to Pd. Ligand **PB1** was found to have an η^3-interaction with the metal center, *via* the phosphorus atom and an η^2-interaction with an aromatic double bond of a mesityl substituent (Fig. 14). A new complex was formed upon addition of PhI, **Pd'-PB1**, in which the ligand was still bound via the phosphorus atom, but now also with a η^4(BCCCH$_2$)-interaction of the mesityl bound boron atom, forming an extended π-coordination. This latter complex showed to be significantly less active in catalysis, and is expected to be a product of decomposition. Analysis of a single crystal by X-ray spectroscopy, and NMR analysis both confirm the formation of **Pd'-PB1**, which was formed via an C-H activation on one of the mesityl rings, resulting in a CH_2 group and loss of 1 equivalent of benzene. An upfield shift of about 10 ppm was found in the ^{11}B NMR spectra, from 69.4 ppm for **Pd-PB1** to 52.8 ppm for **Pd'-PB1**, suggesting the presence of some Pd → B interaction. This structure shows a rare example of a η^4-boratabutadiene complex.

Dalton Transactions Accepted Manuscript

This journal is © The Royal Society of Chemistry 20xx

Please do not adjust margins

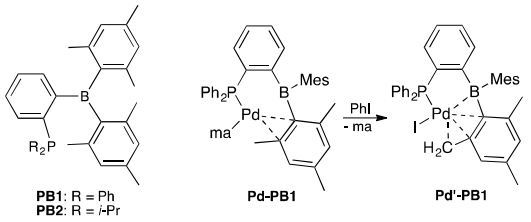

Figure 14. Left: phosphine-borane based ligands as synthesized in the group of Bourissou.[73] Right: Pd based complex **Pd-PB1** and its reaction with PhI to **Pd'-PB1**.

To explore the possibilities of borane-based ligands as supporting ligands in catalysis, the group of Emslie designed multidentate ambiphilic ligands with a phosphine donor and a borane acceptor, aiming for π-coordinating systems. The phosphine-borane based TXPB ligand (Fig. 15a) was designed to anchor the metal center *via* the thioxanthene backbone and explored with a variety of metals, amongst which nickel, palladium and rhodium. The ligand was shown to be versatile and gave rise to a broad variety of complexes, but problems were encountered as the central thioether donor group was shown to be easily replaced from the metal center.[66, 75, 76] Therefore, a new ligand system was designed containing a bisphosphine moiety instead. A ferrocene group was included to provide increased flexibility, while still remaining a firmly bound complex. The ligand FcPPB (FcPPB = Fe(η^5-$C_5H_4PPh_2$)(η^5-$C_5H_4PtBu\{C_6H_4(BPh_2)$-*ortho*$\}$), Fig. 15b) was bound to platinum using $Pt(nb)_3$ (nb = norbornadiene), affording an arylborane complex that binds the two phosphorus atoms, and the borane-phenyl moiety *via* an η^3-BCC interaction with both the *ipso* and *ortho* carbon atoms.[75] Similar structures were obtained when performing the metallation with either $Ni(cod)_2$ or $Pd_2(dba)_3$, resulting in **Ni(FcPPB)** and **Pd(FcPPB)**, respectively, both containing the η^3-BCC interaction with the phenyl-boron moiety.[77]

The reactivity of **Pt(FcPPB)** with small molecules was explored. A CO molecule was bound to the Pt center upon exposure to a CO atmosphere, resulting in **Pt(FcPPB)(CO)**, which was characterized as an FcPPB complex connected to the ligand *via* the two phosphorus atoms and a η^2-BC interaction with the borane moiety, next to a CO molecule. Exposure of **Pt(FcPPB)** to an atmosphere of H_2 afforded **PtH(μ-H)(FcPPB)** by inserting a H in the Pt–B bond and adding the other H to Pt. It was shown that H_2 was only weakly bound, as **Pt(FcPPB)** was regained slowly upon storing the complex under argon and rapidly upon applying vacuum. Furthermore, it was possible to gain **Pt(FcPPB)(CO)** upon exposure to a CO atmosphere, and also its reverse reaction was possible.

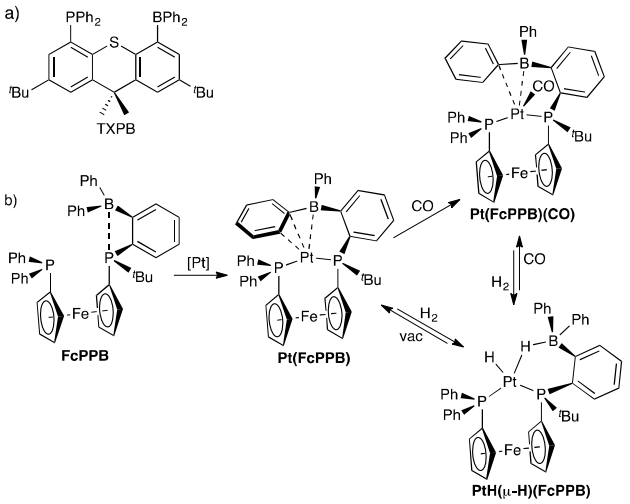

Figure 15. a) TXPB ligand. b) Bisphosphine-ferrocene based ligand FcPPB, the Pt based complexes and their reactivity with CO and H_2.

Ambiphilic, tridentate diphosphanylborane (DPB) ligands, were originally introduced by Bourissou and co-workers in 2006.[78] In their work on rhodium complexes, only the a Rh→B coordination mode was observed. Subsequently, Cu(I) coordination chemistry revealed that this ligand scaffold could also accommodate η^2(BC) or η^3(BCC) coordination modes.[79] Further research on the rhodium system was performed by Ozerov and co-workers, in which the coordination of the borane unit was shown to bind via the π-system of the borabenzyl moiety.[80] Next to this, the product of oxidative addition of the B–C bond was obtained, forming a PBP-pincer complex. The group of Peters explored further possibilities of these ligands. In particular, substitution of the boron-phenyl moiety for the more bulky boron-mesityl group was found to strongly impact the coordination chemistry and the reactivity of the ligand. A nickel-borane complex was formed from a comproportionation reaction with $NiBr_2$ and $Ni(cod)_2$.[81] Analysis by X-ray crystallography showed a coordination of the ($^{Mes}DPB^{Ph}$) ligand *via* the two phosphorus atoms and a η^2(B,C) coordination of the boron atom and the *ipso*-carbon atom of the mesityl ring, next to a bound bromide ligand (**($^{Mes}DPB^{Ph}$)NiBr**, Chart 2). The complex was reduced using Na/Hg resulting in the Ni(0) complex **($^{Mes}DPB^{Ph}$)Ni**, which surprisingly did not bind a solvent molecule. Both of the phosphorus atoms were bound to nickel, as for the Ni(I) complex, but the coordination of the borane substituent changed, as it was now bound in an η^3-BCC fashion, also binding the *ortho*-carbon atom of the mesityl ring. Whereas a previously synthesized phenyl analogue **($^{Ph}DPB^{Ph}$)Ni(THF)** did not show any activity towards H_2, **($^{Mes}DPB^{Ph}$)Ni** showed facile heterolytic activation of the substrate at room temperature in C_6D_6. The hydrogen-bound complex was identified as the hydrido-borohydrido species **($^{Mes}DPB^{Ph}$)(μ-H)NiH**, as shown in Chart 2, and was found to be in a 5:1 equilibrium with **($^{Mes}DPB^{Ph}$)Ni**. Similar activity was found when the iron-CO analogue **($^{Ph}DPB^{Ph}$)Fe(CO)$_2$** was exposed to 1 atm of H_2, forming **($^{Ph}DPB^{Ph}$-H)Fe(H)(CO)$_2$**, in which the hemilabile η^3-BCC

Dalton Transactions Accepted Manuscript

Please do not adjust margins

interaction participated and hydrogen was added in a heterolytic manner.[82]

The catalytic possibilities of **(^{Mes}DPB^{Ph})Ni** were investigated by addition of styrene under a H_2 atmosphere, after which the hydrogenated product ethyl benzene was formed directly. The reaction was monitored by ^{1}H NMR spectroscopy, showing that the starting complexes were again present in an equilibrium with H_2 after full consumption of the substrate, showing that the catalyst could be recovered after catalysis.[81]

Further exploration of **(^{Mes}DPB^{Ph})Ni** in catalytic reactions showed that it is an efficient catalyst for the hydrosilylation of *para*-substituted benzaldehydes with diphenylsilane, *via* the formation of a borohydrido-Ni-silyl species in which $SiHPh_2$ is bound to nickel and the hydride is inserted in the B-Ni bond.[83]

Synthesis of the phenyl substituted P^{i}Pr$_2$ analogue **(^{Ph}DPB^{iPr})Ni** showed reactivity toward H_2 as well.[84] The introduction of the more electron-rich *iso*-propyl substituent in combination with the less bulky phenyl ring on boron tuned the geometric and electronic environment such that the observation of the hydrogen adduct was possible. This unusual Ni-(H_2) complex subsequently reacted to form a similar hydrido-borohydrido species, forming **(^{Ph}DPB^{iPr})(μ-H)NiH**.

Similar binding modes for the DPB scaffold also play a role in iron-mediated dinitrogen functionalization. The dinitrogen-bridged di-iron complex **(^{Ph}DPB^{iPr})Fe(μ-1,2N$_2$)Fe(^{Ph}DPB^{iPr})**[85] could be functionalized by addition of 1,2-bis(chlorodimethylsilyl)ethane (bse) and 2.1 equivalents of Na/Hg under 1 atm of N_2, forming **(^{Ph}DPB^{iPr})Fe(N$_2$bse)**. This new complex formed an η^3(B,C,C)-interaction with the iron center and the phenyl substituted borane tether. Activation of phenylsilane was performed by hydrosilylation of the Fe-N bond, placing SiH_2Ph to Nα and H to B. Similar reactivity was found for the Co analogue **(^{Ph}DPB^{iPr})Co(N$_2$)**, and the substrate scope was extended with both, the iron and cobalt nitrogen bound complexes.[86]

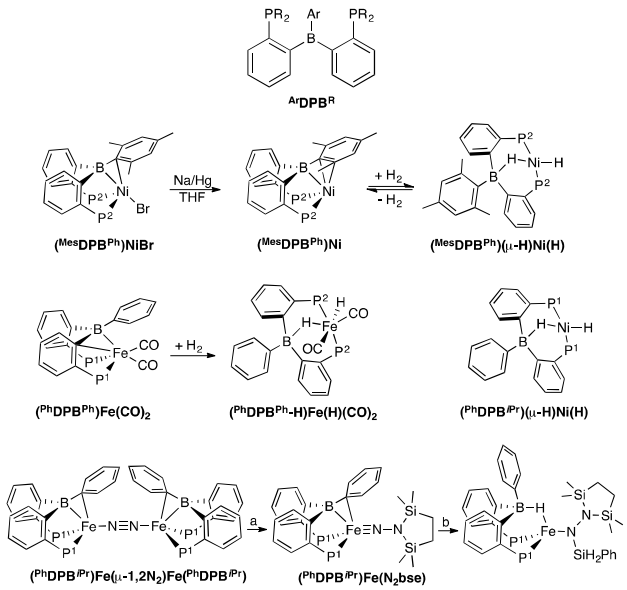

Chart 2. Selected DPB complexes. P = P^1 or P^2; P^1 = iPr, P^2 = Ph; R = Ph or iPr; Ar = Mes or Ph; a = 1,2-bis(chlorodimethylsilyl)ethane, 2.1 equiv Na/Hg, 1 atm of N_2, b = $PhSiH_3$.

Stephan and co-workers developed ruthenium-based systems containing the ^{ph}DPB^{ph} ligand.[87] The ligand was bound to Ru *via* both phosphorus atoms and an interaction with the phenyl substituent on the borane, forming a positively charged complex with a $B(C_6F_5)_4$ counterion, i.e. **[(^{ph}DPB^{ph})RuCl]B(C_6F_5)$_4$**. The complex showed reactivity upon addition of PCy_3, binding the phosphorus atom to the interacting phenyl ring on its *ortho*-position, resulting in the cyclohexadienyl (chd) containing Ru-complex **(^{chd}DPB^{ph})Ru(PCy$_3$)Cl]B(C_6F_5)$_4$**. A subsequent reaction was observed upon exposure to H_2, activating it in a heterolytic fashion and cleaving the C_{Ar}-PCy_3 bond. The resulting neutral cyclohexadienyl complex was found to be present in two isomers, with an *ortho* or a *para* addition at the arene ring. **[(^{ph}DPB^{ph})RuCl]B(C_6F_5)$_4$** was explored in the hydrogenation of imines, which were shown to proceed at room temperature under high pressures of H_2 (102 atm, 1-10 mol% cat, 83-99% yield). The proposed mechanism proceeds *via* the previously synthesized complex **(^{chd}DPB^{ph})RuCl**, both the *ortho* or a *para* form. This is consistent with an FLP-type (FLP = frustrated Lewis pair) hydrogenation in which the complex and the substrate act as an FLP to split H_2. The cleaved hydrogen is subsequently delivered to the formed iminium cation (Fig. 16).

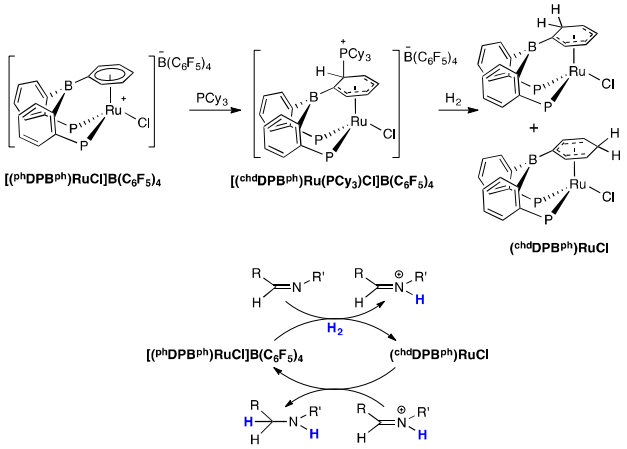

Figure 16. (DPB)Ru structures and its mechanism for the hydrogenation of imines. P = Ph$_2$; R = Ph, R' = ^{t}Bu or Ph.

These examples show the versatility that incorporation of borane ligands can bring to the coordination chemistry *via* their extended π-system, leading to various coordination modes making them excellent adaptive ligands. The resulting complexes are shown to be active toward small molecule activation *via* a heterolytic pathway transiently accepting hydrides either at the boron site or at a remote carbon site of the conjugated aromatic ring as demonstrated in the last example.

4 π-Bound C=E bonds

In comparison with olefins, the C=E (E = O or N) bond of carbonyls and imines becomes both polar and electron deficient because of the high electronegativity of the element

This journal is © The Royal Society of Chemistry 20xx

Dalton Transactions Accepted Manuscript

Please do not adjust margins

E. Hence, the backdonation interaction is expected to play a dominant role in the description of π-bound C=E bonds. In addition, the presence of lone pairs on the heteroelement may open up reactive pathways that are not accessible to C=C bonds.

Polar C=E bonds can bind to the metal center in either an η^1(E) or η^2(C,E)-fashion, the former being by far the most common mode. Here we discuss situations in which the latter (π-coordination) is favored. The incorporation of a carbonyl will be discussed first, followed by the incorporation of imine and iminium moieties.

4.1 Carbonyl complexes

Carbonyl groups (i.e. aldehydes and ketones) are known to bind to a metal center in two distinct ways, i.e. η^1(O) to electrophilic metals, by donation of the oxygen lone pair to the metal center, and η^2(C,O) to electron-rich metals. The latter case is stabilized by π-backdonation of the metal to the ligand, creating a stronger M–L bond and a weakening of the C=O bond, in line with the binding mode of alkene systems. The C=O interaction can be described by two resonance extremes; the side-on bound extreme and the metallaoxacycle extreme (Fig. 17). Cooperative behavior in such systems can be envisioned arising from the labile (C=O)–M bond, creating the possibility of a hemilable system. Activation of a small molecule can proceed *via* heterolytic activation, adding part of the substrate to the oxygen of the ligand backbone and part to the metal center, provided that the carbonyl moiety has an η^2(C,O) interaction with the metal center. In general, this interaction is scarcely found compared to the η^1(O) bound structure, but it is found more commonly for electron rich systems which can efficiently back donate.[39]

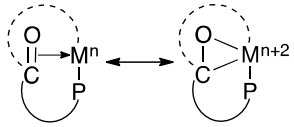

Figure 17. Resonance extremes of an η^2-bound ketone-metal interaction, left: the side-on adduct, right: the metalaoxo-cycle in which the oxidation state is raised by 2.

An early example of a pincer-type ligand incorporating an η^2-coordinating ketone was developed in the group of Milstein. The synthesis and characterization of an iridium complex containing a quinone-based ligand was reported.[88] The ligand was designed with phosphorus groups attached at the *ortho* positions to bind the metal center in a multidentate fashion. Upon synthesis of a cationic complex, a bond between the iridium center and the phosphorus groups was obtained, as well as an interaction with the *ipso* C=O group, establishing the first stable phenoxonium complex (Fig. 18a). The C=O moiety was bound via an η^2-coordination to the metal, resulting in a stabilized cationic ligand. It was shown that the positive charge was mainly delocalized over the aromatic ring. An X-ray single crystal structure was obtained for the acetonitrile bound PCOP-complex (Fig. 18b). The bond angles inside the ring were found to be close to 120°, of which it was concluded that the system is best described as an Ir(I) complex with a C=O double-bond coordination compared to the Ir(III) three-centered metalaoxa-cycle structure.[88]

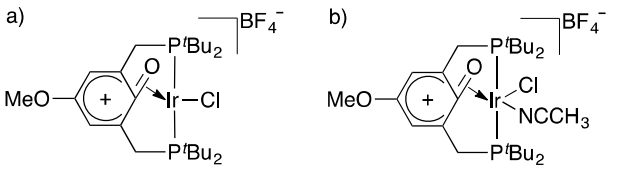

Figure 18. a) The pincer-type quinone based iridium complex and b) the acetonitrile bound analogue of which an X-ray single crystal structure was obtained.

A somewhat analogous structure was obtained by Piers and coworkers[89] from the reaction of a pincer type iridium $PC_{sp2}P$ with N_2O to form an iridaepoxide complex. The C=O moiety was formed by exposure of the carbene chloride complex to N_2O, by addition of an oxygen atom to the Ir=C bond, cleanly synthesizing the iridium complex containing the η^2-coordinated C=O moiety (Fig. 19). The iridaepoxide shows a moderate upfield shift at 65 ppm in ^{13}C NMR. X-ray crystal structure analysis showed a C–O distance of 1.350(7) Å, which is in between a C–O double and single bond, i.e. ~1.21 Å and ~1.45 Å. An Ir–O distance of 2.034(4) Å was found and an Ir–C distance of 2.080(6) Å, both in the range of a single bond.

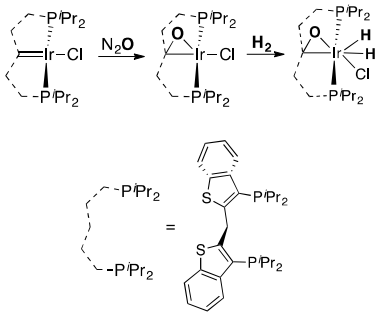

Figure 19. Schematic representation of the pincer type iridium $PC_{sp2}P$ iridium complex and its reaction with N_2O, forming the iridaepoxide complex, and the following reaction with H_2 (top) and the schematic and chemical representation of the ligand (bottom).

Hydrogen binds to the iridium center upon exposure of the iridaepoxide to 1 atm H_2 at room temperature, from which H_2O is subsequently eliminated. The mechanism of this formal hydrogenation of N_2O was investigated in detail, in which it was proposed that this elimination occurs via migration of a proton to the oxygen atom, forming an alcohol group on the carbene carbon atom and a hydride on the iridium center, as shown in Fig. 20a.[90] This step can either be seen as a reductive elimination/oxidative addition mechanism when starting from the iridaepoxide extreme, or as a 1,2-insertion/β-elimination when starting from the η^2-coordinated C=O extreme (Fig. 20b). In a next step the alcohol group migrates to iridium and H_2O is eliminated.[90] In this proposed mechanism the metal-ligand system operates in a truly cooperative fashion, storing part of the activated small molecule on the ligand backbone.

Dalton Transactions Accepted Manuscript

Please do not adjust margins

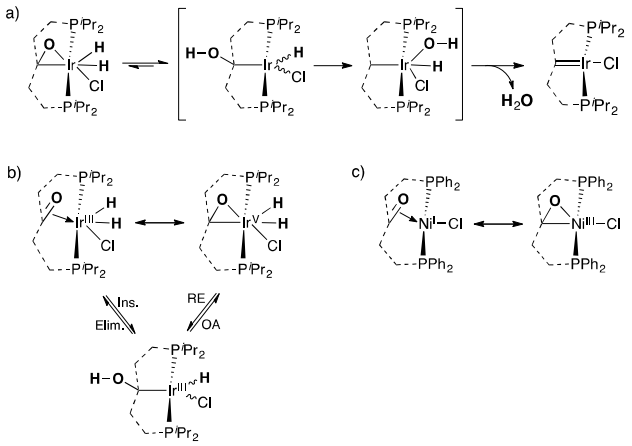

Figure 20. a) The iridaepoxide complex with one equivalent of H_2 added and the following H_2O elimination pathway. The ligand is represented schematically as in Figure 19. b) Resonance structures of the hydrogen bound iriudium complex and the visualization of the proton migration, starting from either Ir(III) or Ir(V) as described by Piers.[90] c) Resonance structures for the (^{ph}dpbp)NiCl complex as described by Moret (*vide infra*).[91]

A more direct synthetic access to supported metallaepoxide structures is provided by the 2,2'-bis(diphenylphosphine)benzophenone (^{ph}dpbp) ligand.[91] The use of ^{ph}dpbp as a chiral ligand was first explored in the group of Ding, where Ru(II)-based Noyori-type systems were developed to perform hydrogenation reactions. The benzophenone backbone was found to induce enantioselectivity in the catalytic hydrogenation of aromatic systems, in which the coordination of the C=O moiety is believed to be the key feature to obtain high yields and selectivity.[92] Our group further explored the chemistry by coordination of ^{ph}dpbp to nickel in the oxidation states of 0, 1 and 2 (Fig. 21). It was found that the ligand ketone moiety does not bind to the metallic center in the high-spin Ni(II) complex **(^{ph}dpbp)NiCl$_2$** (Ni–C: 3.4031(12) Å, Ni–O: 3.1012(10) Å), but this interaction was induced by reduction of the complex. The synthesis of **(^{ph}dpbp)Ni(I)Cl** and **(^{ph}dpbp)Ni(0)PPh$_3$** both lead to a η^2(C,O) interaction, leading to shorter bond distances between the ketone moiety and the metallic center (Ni–C: 2.006(2) Å, Ni–O: 1.9740(15) Å for Ni(I) and Ni–C: 2.001(2) Å, Ni–O: 2.0091(14) Å for Ni(0)). Next to this, the C=O bond was elongated from 1.213(3) Å in the Ni(II) structure to 1.310(2) Å in the Ni(I) and 1.330(3) Å in the Ni(0) structure, showing significant π-backdonation from the metal to the C=O moiety in the latter two cases (Fig. 22). NBO analysis of a DFT-computed electron density revealed an increased negative charge on the C=O fragment of –0.5e and –0.6e upon binding to Ni(I)Cl and Ni(0)PPh$_3$, respectively. This additionally supports the predominantly electron accepting nature of the ketone moiety, which can be seen to function as a hemilabile acceptor ligand.[91]

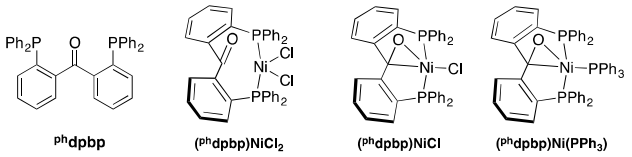

Figure 21. Left-to-right: Diphosphine-ketone ligand 2,2'-bis(diphenylphosphine)-benzophenone (^{ph}dpbp), and the metal complexes **(^{ph}dpbp)NiCl$_2$**, **(^{ph}dpbp)NiCl** and **(^{ph}dpbp)Ni(PPh$_3$)**.

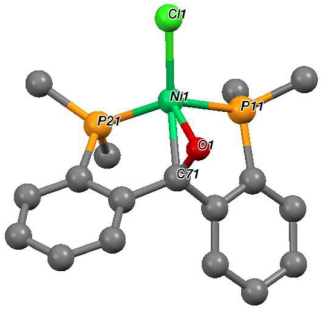

Figure 22. Crystal structure of **(^{ph}dpbp)NiCl** showing the η^2(C,O) interaction with the nickel center, phenyl groups on the phosphorus atoms are omitted for clarity except for the bound carbon atom.

In a related study, Ruhland and co-workers explored the use of bisphosphinite ligands for the activation of unstrained C(sp^2)-C(sp^2) bonds. Coordination of the bisphosphinite ligand (^{iPr}dpobp, Fig. 23) to nickel,[93] rhodium[94] or iridium[95] resulted in quantitative oxidative addition of the PhC–(CO) bond, breaking the ligand backbone. This reaction is proposed to proceed *via* a η^2(C,O) interaction of the ketone moiety. Such pathways were not observed when using ^{ph}dpbp as the ligand, suggesting that the tether length is of importance to the stability of η^2(C,O) complexes.

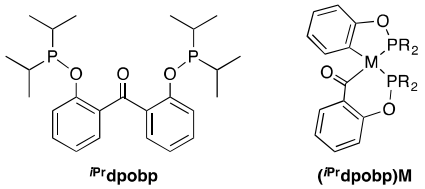

Figure 23. Bisphosphite ligand ^{iPr}dpobp and the metal complexes. M = Ni, Rh, Ir; R = *i*Pr.

Coordination of a phosphine-tethered aldehyde ligand was explored in the group of Yeh. The bidentate P,O-chelating ligand *o*-(diphenylphosphine)benzaldehyde (PCHO) in combination with group 6 metals Mo[96] and W[97] was described. A complex with an octahedral geometry around the metal center was synthesized in both cases, binding two PCHO ligands and two CO ligands (Fig. 24a). The aldehyde moieties were shown to bind to the metal center in a η^2-fashion by elongation of the aldehyde C=O bonds upon complexation due to π-backbonding to the empty π*-orbital of this fragment (Mo, C–O: 1.335(4) Å and 1.323(4) Å; W, C–O: 1.338(5) Å and 1.357(5) Å). A distinctive shift of the furan proton was observed in ^{1}H NMR, from 10.50 ppm in the free PCHO ligand to 5.38 ppm in case of Mo and 5.12 ppm in case of W. The

This journal is © The Royal Society of Chemistry 20xx
Please do not adjust margins
Dalton Transactions Accepted Manuscript

phosphorus signal was shown to shift from -11.37 ppm in the free PCHO ligand to 18.04 ppm for Mo and 10.03 ppm for W. The reactivity of the molybdenum complex **Mo(PCHO)$_2$(CO)$_2$** with C_{60} was explored: the formed molybdenum complex still contained two CO ligands next to C_{60}, the latter being bound in an η^2-fashion through a 6:6-ring junction. Furthermore, the two bound PCHO ligands unexpectedly reacted, forming a *trans*-stilbene type ligand, bound via the carbon-carbon double bond in the backbone as well as the phosphorus ligands, resulting in **Mo(PCH=CHP)(CO)$_2$(C$_{60}$)** (Fig. 24b). This binding is similar to the *trans*-stilbene type ligands shown in section 2.1 (*vide supra*). Analysis by single crystal X-ray diffraction showed an η^2-bound C=C moiety with a bond length of 1.418(7) Å, which is in the range of the olefinic C–C bonds of the described *trans*-stilbene type ligands that were found to be between 1.40 Å and 1.44 Å.[96]

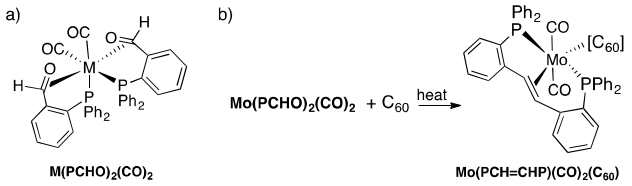

Figure 24. a) Octahedral complexes M(PCHO)$_2$(CO)$_2$, M = Mo or W, PCHO = *o*-(diphenylphosphine)benzaldehyde. b) Activity study of **Mo(PCHO)$_2$(CO)$_2$** with C_{60}, resulting in the trans-stilbene complex **Mo(PCH=CHP)(CO)$_2$(C$_{60}$)**.

4.2 Imine complexes

Imines are ubiquitous as ligands for transition metals, forming σ dative bonds by donation of one of the lone pairs of the nitrogen atom. Because this binding mode is generally preferred, π-complexes of C=N bonds are rare (Fig. 25). Here we discuss recent examples where this binding mode is accessed upon formal deactivation of the N-centered lone pair either by coordination to another metal or by substitution to generate an iminium cation.

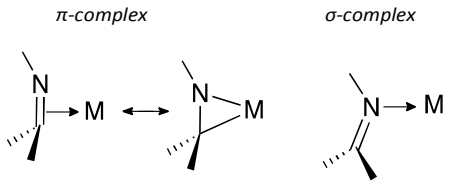

Figure 25. Left: Schematic representation of the two resonance extremes of a imine π-complex, right: representation of the imine σ-complex.

A rhodium based amido-bridged dinuclear complexes was synthesized in the group of de Bruin, **[Rh(nbd)$_2$(μ-bpa)]Cl** (nbd = norbornadiene, bpa = bis(2-picolyl)amine).[98] The complex was shown to be susceptible to deprotonation by KO^{t}Bu, resulting in the complex **Rh(nbd)$_2$(μ-bpi)**, where the doubly deprotonated bis(2-picolyl)amine (PyCH$_2$NHCH$_2$Py, bpa) ligand is transformed to a neutral PyCH=N-CH$_2$Py (bpi) ligand containing an imine functionality (Fig. 26a). The two complexes are related by acid-base chemistry, as the backward reaction is possible by protonation with NHEt$_3$Cl. Both the C and N atom of the deprotonated complex have a trigonal geometry, suggesting the formation of a π-coordinating imine C=N fragment (Fig. 26b). Next to this, the C–N distance was found to be shorter upon comparison to the protonated complex, i.e. 1.415(4) Å *versus* 1.482(6) Å, respectively. In agreement with further analysis, this complex was described as a mixed valence Rh(-1,1) complex. The complex reacted rapidly with oxygen in benzene, leading to new, mononuclear complexes.[98] Analogues to this rhodium complex, the synthesis of another group 9 binuclear complex was explored using iridium (Fig. 26c).[99] An X-ray crystal structure of the cationic complex **[Ir(nbd)$_2$(μ-bpi)]PF$_6$** was obtained, showing a similar complex as the rhodium analogue. The rather unusual bridging π-coordination was again obtained, which was described as the first example of a π-bound imine moiety for iridium. Both of the iridium centers in the complex bind to the imine moiety, of which one adopts a σ-coordination to the imine nitrogen atom, activating the imine for η^2-coordination to the other iridium center. Next to this, both iridium centers also bear a cod ligand. The η^2-bound imine was shown to gain substantial π-backdonation, as the C-N bond has a length of 1.407(3) Å which is substantially longer compared to σ-coordinated imines to iridium that have a typical length of ~1.30 Å.[99] As a result it can be concluded that both resonance extremes play a role in binding, i.e. the side-on bound Ir(I) extreme and the Ir(III) irida-aza-cyclopropane extreme (Fig. 26d). The iridium complex was shown to be an active pre-catalyst for water oxidation after treatment with cerium ammonium nitrate (Ce^{IV}) as the oxidant.[99] The research using the bpi ligand was extended to the use of mixed metal systems. Complexes with Rh-Ir[100] and Pd-Ir[101] were synthesized, which both still contained the η^2-bound imine moiety.

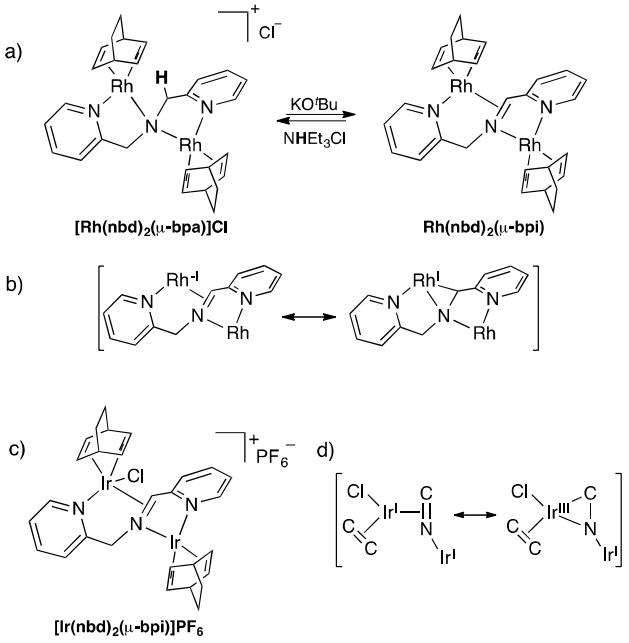

Figure 26. a) Rh-based complexes and their acid-base chemistry. b) Resonance extremes of the Rh-imine bound structure. c) Structure of the cationic Ir-based complex. d) Resonance extremes of the Ir-imine bound structure. Figure adapted from de Bruin.[98, 99]

Dalton Transactions Accepted Manuscript

Other rhodium complexes with an η^2-bound N=C double bond have been synthesized from a bulky $trop_2NMe$ ligand (trop = 5H-dibenzo[a,d]cyclohepten-5-yl).[102, 103] They were formed in multiple steps, starting from $trop_2NMe$, $Rh(\mu_2\text{-}Cl)_2(cod)_2$ and PPh_3, resulting in **$Rh(trop_2NMe)(PPh_3)$** which was further reacted with AgOTf to yield the positively charged complex **$[Rh(trop_2NMe)(PPh_3)]OTf$**. The methyl group was subsequently deprotonated with KO^tBu to form an interaction between C_{Me} and Rh, forming an unsaturated C=N ligand (**$Rh(trop_2N{=}C)(PPh_3)$**) (Fig. 27a,b). The binding of this moiety can either be considered as a rhodaazacyclopropane or as the η^2-side-on bound (C=N)–M complex (Fig. 27c). The N–CH_2 distance is 1.446(5) Å, which is significantly shorter compared to the N–CH_3 which was found to be 1.505(7) Å, but on the other hand longer then other C=N bonds in iminium ions (1.274-1.301 Å). The rhodaazacyclopropane description has an energetically low-lying π*-orbital of the N-C bond, and so π-backdonation to the ligand is strong. For these reasons in combination with further analysis by NMR, the metallacycle description is the most accurate for this complex. The properties of **$Rh(trop_2N{=}C)(PPh_3)$** were explored with cyclic voltammetry in a THF solution, in which the complex could be oxidized. The **$Rh(trop_2N{=}C)(PPh_3)^{\cdot+}$** complex was stable enough to be analyzed by EPR spectroscopy, from which it was shown that the structural features of the starting complex were retained, obtaining a rhodaazacyclopropyl radical cation. In analogy to the neutral complex, this complex is also best described as a RhNC metallacycle (Fig. 27c), showing the possibility of this ligand to stabilize multiple oxidation states with a single geometry.[103]

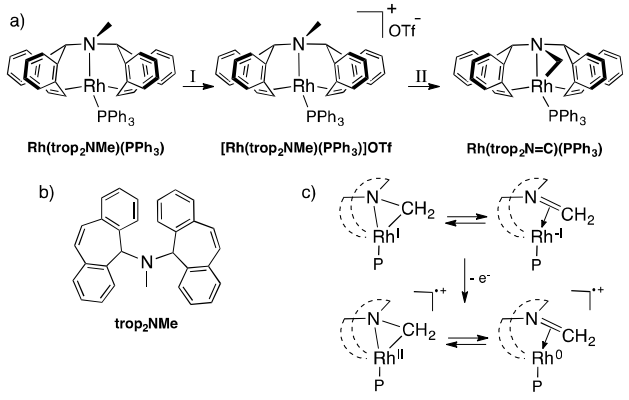

Figure 27. a) Synthesis of Rh-based complexes, I = AgOTf ; II = KO^tBu. b) The ligand $trop_2NMe$. c) Binding modes of **$Rh(trop_2N{=}C)(PPh_3)$** and **$Rh(trop_2N{=}C)(PPh_3)^{\cdot+}$**, the rhodaazacyclopropane and the η^2-side-on bound (C=N)–M complex.

Conclusions

The inclusion of π-coordinating ligands in organometallic complexes is a versatile tool to induce metal-ligand cooperativity. The recent advances described here illustrate how the reactivity of metal-bound π-systems can be controlled by ligand design. In particular, the incorporation of a variety of tethers to connect the π-coordinating moiety and additional donor groups, mainly based on coordinating P-donors, exerts a strong influence on its coordination mode and reactivity. In the arene based chemistry, the tether length can favor or disfavor coordination of the aromatic π-system: the long, flexible tether in (^{ph}PArP)Rh complexes combined with steric encumbrance turns a strong η^6-arene ligand into a hemilabile moiety. Conversely, the rigid *ortho*-phenylene tethers in terphenyl-based ligands impose a close proximity between an aromatic moiety and group 10 metals.

The use of rigid tethers also stabilize unusual coordination modes of certain π-systems, such as the side-on coordination of the C=O moiety in Milstein's quinone based iridium pincer complexes. Similarly, the *ortho*-phenylene tethers in ketone-based pincer ligands favor the η^2(CO) binding mode over the η^1(O), resulting in hemilabile-acceptor behavior in (^{ph}dpbp)NiL complexes. Another striking example of tether-imposed binding mode is the unusual coordination mode of the pyridine moiety in Ni(PPyP) complexes: the anchoring of the phosphorus groups on the *meta* positions leads to the nickel center coordinating a C=C bond of the aromatic ring, whereas a pyridine ring usually coordinates via its nitrogen atom lone pair. Due to this binding mode, an electron deficient aromatic ring could be generated *via* coordination of Lewis-acidic borane ligand to the lone pair on the pyridine nitrogen atom, leading to enhanced hydride affinity and allowing for bifunctional activation of silanes and boranes.

This last example also illustrates how reactivity at π-ligands can be tuned by electronic effects. Related reactivity was observed upon introduction of electron-deficient borane substituents. Interaction of arylborane moieties with reduced metal centers often involves both the boron atom and the aromatic system in η^2(BC) or η^3(BCC) coordination modes, as featured in the chemistry of diphosphine-borane (DPB) ligands. Cooperative reactivity of DPB complexes usually involves the boron center functioning as a hydride acceptor, allowing for the activation of a range of small molecules by iron, cobalt, and nickel compounds. Remarkably, a high hydride affinity at the boron-substituted aromatic ring has also been observed in ruthenium chemistry of the ^{ph}DPB^{ph} ligand: a hydride can be incorporated on the carbon-backbone of the ligand, allowing the η^6-bound arene moiety in **$[(^{ph}DPB^{ph})RuCl]^+$** to function as a hydride acceptor in frustrated Lewis pair chemistry.

Metal-ligand cooperation is a versatile tool in current efforts to transition from precious to base metals in catalysis. The recent advances discussed herein highlight the incorporation of tethered π-ligands as a promising strategy for the design of new and tuneable cooperative systems, hopefully stimulating further development of this class of compounds for base metal catalysis.

Acknowledgements

The authors would like to thank the Sectorplan Natuur- en Scheikunde (Tenure-track grant at Utrecht University) for financial support.

Dalton Transactions Accepted Manuscript

This journal is © The Royal Society of Chemistry 20xx

Notes and references

1 J. I. van der Vlugt, *Eur. J. Inorg. Chem.*, 2012, 363–375.
2 J. R. Khusnutdinova, D. Milstein, *Angew. Chem. Int. Ed.*, 2015, **54**, 12236–12273.
3 P. J. Chirik and K. Wieghardt, *Science* 2010, **327**, 794–795.
4 J. C. Jeffrey, T. B. Rauchfuss, *Inorg. Chem.*, 1979, **18**(10) 2658–2666.
5 P. Braunstein, F. Naud, *Angew. Chem. Int. Ed.*, 2001, **40**, 680–699.
6 W. I. Dzik, J. I. van der Vlugt, J. N. H. Reek, B. de Bruin, *Angew. Chem. Int. Ed.*, 2011, **50**, 3356–3358.
7 O.R. Luca and R.H. Crabtree, *Chem. Soc. Rev.*, 2013, **42**, 1440–1459.
8 P. J. Chirik, *Inorg. Chem.*, 2011, **50**, 9737–9740.
9 T. W. Myers, L. A. Berben, *J. Am. Chem. Soc.*, 2011, **133**, 11865–11867.
10 T. W. Myers, L. A. Berben, *J. Am. Chem. Soc.*, 2013, **135**, 9988–9990.
11 R. Noyori, *Angew. Chem. Int. Ed.*, 2002, **41**, 2008–2022.
12 E. Balaraman, C. Gunanathan, J. Zhang, L. J. W. Shimon, D. Milstein, *Nat. Chem.*, 2011, **3**, 609−614.
13 S. P. Semproni, C. Milsmann, P. J. Chirik, *J. Am. Chem. Soc.*, 2014, **136**, 9211−9224.
14 R. Langer, G. Leitus, Y. Ben-David, D. Milstein, *Angew. Chem. Int. Ed.*, 2011, **50**, 2120–2124.
15 Y. Shvo, D. Czarkie, Y. Rahamim, *J. Am. Chem. Soc.*, 1986, **108**, 7400–7402.
16 J. Pearson, R. J. Shively, Jr., R. A. Dubbert, *Organometallics* 1992, **11**, 4096–4104.
17 H.-J. Knölker, E. Baum, R. Klauss, *Tetrahedron Lett.*, 1995, **36**, 7647–7650.
18 C. P. Casey, H. Guan, *J. Am. Chem. Soc.*, 2007, **129**, 5816–5817.
19 B. L. Conley, M. K. Pennington-Boggio, E. Boz, T. J. Williams, *Chem. Rev.*, 2010, **110**, 2294–2312.
20 I. Bauer, H-J. Knölker, *Chem. Rev.*, 2015, **115**, 3170–3387.
21 P. E. Sues, K. Z. Demmans, R. H. Morris, *Dalton Trans.*, 2014, **43**, 7650–7667.
22 S. Chakraborty, P. O. Lagaditis, M. Förster, E. A. Bielinski, N. Hazari, M. C. Holthausen, W. D. Jones, S. Schneider, *ACS Catal.*, 2014, **4**, 3994−4003.
23 R. Langer, M. A. Iron, L. Konstantinovski, Y. Diskin-Posner, G. Leitus, Y. Ben-David, D. Milstein, *Chem. Eur. J.*, 2012, **18**, 7196–7209.
24 N. Gorgas, B. Stöger, L. F. Veiros, E. Pittenauer, G. Allmaier, K. Kirchner, *Organometallics* 2014, **33**, 6905−6914.
25 S. Chakraborty, H. Dai, P. Bhattacharya, N. T. Fairweather, M. S. Gibson, J. A. Krause, H. Guan, *J. Am. Chem. Soc.*, 2014, **136**, 7869−7872.
26 J. I. van der Vlugt, J. N. H. Reek, *Angew. Chem. Int. Ed.*, 2009, **48**, 8832–8846.
27 S. Schneider, J. Meiners, B. Askevold, *Eur. J. Inorg. Chem.*, 2012, 412–429.
28 C. Gunanathan, D. Milstein, *Acc. Chem. Res.*, 2011, **44**(8), 588–602.
29 V. Lyaskovskyy and B. de Bruin, *ACS Catal.* 2012, **2**, 270−279.
30 M. Asay, D. Morales-Morales, *Dalton Trans.*, 2015, **44**, 17432–17447.
31 G. van Koten, D. Milstein, Topics in Organometallic Chemistry, *Organometallic Pincer Chemistry*, Springer, 2013.
32 A. M. Tondreau, C. C. Hojilla Atienza, K. J. Weller, S. A. Nye, K. M. Lewis, J. G. P. Delis, P. J. Chirik, *Science* 2012, 567–570.
33 D. Morales-Morales, C. M. Jensen, *The Chemistry of Pincer Compounds*, Elsevier Science, Amsterdam, 2007.
34 K. J. Szabó, O. F. Wendt, *Pincer and Pincer-Type Complexes*, Wiley-VCH, Weinheim, 2014.
35 M. Albrecht, G. van Koten, *Angew. Chem. Int. Ed.*, 2001, **40**, 3750–3781.
36 M. E. van der Boom, D. Milstein, *Chem. Rev.*, 2003, **103**, 1759–1792.
37 M. W. O'Reilly, A. S. Veige, *Chem. Soc. Rev.*, 2014, **43**, 6325–6369.
38 W. C. Zeise, *Poggendorffs Ann. Phys.*, 1827, **9**, 632-633.
39 R. H. Crabtree, *The organometallic chemistry of the transition metals*, Fifth edition, Wiley, New Haven, 2009.
40 M. A. Bennett, P. W. Clark, *J. Organomet. Chem.*, 1976, **100**, 367–381.
41 M. A. Bennett, R. N. Johnson, I. B. Tomkins, *J. Organomet. Chem.*, 1976, **118**, 205–232.
42 W. Baratta, E. Herdtweck, P. Martinuzzi, P. Rigo, *Organometallics* 2001, **20**, 305–308.
43 B. J. Barrett, V. M. Iluc, *Organometallics* 2014, **33**, 2565–2574.
44 B. J. Barrett, V. M. Iluc, *Inorg. Chem.*, 2014, **53**, 7248–7259.
45 C. C. Comanescu, M. Vyushkova, V. M. Iluc, *Chem. Sci.*, 2015, **6**, 4570–4579.
46 A. V. Polukeev, R. Marcos, M. S. G. Ahlquist, O. F. Wendt, *Chem. Sci.*, 2015, **6**, 2060–2067.
47 a) A. Friedrich, R. Ghosh, R. Kolb, E. Herdtweck, S. Schneider, *Organometallics* 2009, **28**, 708–718; b) C. Bianchini, E. Farnetti, M. Graziani, G. Nardin, A. Vacca, F. Zanobini, *J. Am. Chem. Soc.*, 1990, **112**, 9190–9197.
48 A. V. Polukeev, O. F. Wendt, *Organometallics* 2015, **34**, 4262–4271.
49 K. J. Jonasson, A. V. Polukeev, R. Marcos, M. S. G. Ahlquist, O. F. Wendt, *Angew. Chem. Int. Ed.*, 2015, **54**, 9372–9375.
50 L. Zhang, T. Yan, Y-F Han, F. E. Hahn, G-X Jin, *Dalton trans.*, 2015, **44**, 8797–8800.
51 K. Okamoto, Y. Omoto, H. Sano, K. Ohe, *Dalton Trans.*, 2012, **41**, 10926–10929.
52 F. M. Dixon, J. R. Farrell, P. E. Doan, A. Williamson, D. A. Weinberger, C. A. Mirkin, C. Stern, C. D. Incarvito, L. M. Liable-Sands, L. N. Zakharov, A. L. Rheingold, *Organometallics* 2002, **21**, 3091–3093.
53 F. M. Dixon, M. S. Masar III, P. E. Doan, J. R. Farrell, F. P. Arnold Jr., C. A. Mirkin, C. D. Incarvito, L. N. Zakharov, A. L. Rheingold, *Inorg. Chem.*, 2003, **42**(10), 3245–3255.
54 R. C. Smith, J. D. Protasiewicz, *Organometallics* 2004, **23**, 4215–4222.
55 B. P. Morgan, R. C. Smith, *J. Organomet. Chem.*, 2008, **693**, 11–16.
56 K. T. Horak, A. Velian, M. W. Day, T. Agapie, *Chem. Commun.*, 2014, **50**, 4427–4429.
57 K. T. Horak, S. Lin, J. Rittle, T. Agapie, *Organometallics* 2015, **34**, 4429–4432.
58 J. T. Henthorn, S. Lin, T. Agapie, *J. Am. Chem. Soc.*, 2015, **137**, 1458–1464.
59 K. T. Horak, T. Agapie, *J. Am. Chem. Soc.*, 2016, **138**, 3443–3452.
60 J. A. Buss, T. Agapie, *Nature* 2016, **529**, 72–75.
61 A. Velian, S. Lin, A. J. M. Miller, M. W. Day, T. Agapie, *J. Am. Chem. Soc.*, 2010, **132**, 6296–6297.
62 S. Lin, M. W. Day, T. Agapie, *J. Am. Chem. Soc.*, 2011, **133**, 3828–3831.
63 K. T. Horak, D. G. VanderVelde, T. Agapie, *Organometallics* 2015, **34**, 4753–4765.
64 G. A. Edouard, P. Kelley, D. E. Herbert, T. Agapie, *Organometallics* 2015, **34**, 5254–5277.
65 M. L. H. Green, *J. Organomet. Chem.*, 1995, **500**, 127–148.
66 D. J. H. Emslie, B. E. Cowie, S. R. Oakley, N. L. Huk, H. A. Jemkins, L. E. Harrington, J. F. Britten, *Dalton Trans.*, 2012, **41**, 3523–3535.
67 A. F. Hill, G. R. Owen, A. J. P. White, D. J. Williams, *Angew. Chem. Int. Ed.*, 1999, **38**(18), 2759–2761.

Dalton Transactions Accepted Manuscript

68 G. Bouhadir, D. Bourissou, *Chem. Soc. Rev.*, 2016, **45**, 1065–1079.
69 A. Amgoune, D. Bourissou, *Chem. Commun.*, 2011, **47**, 859–871.
70 H. Braunschweig, R. D. Dewhurst, *Dalton Trans.*, 2011, **40**, 549–558.
71 I. Kuzu, I. Krummenacher, J. Meyer, F. Armbruster, F. Breher, *Dalton Trans.*, 2008, **43**, 5836–5865.
72 D. J. H. Emslie, B. E. Cowie, K. B. Kolpin, *Dalton Trans.*, 2012, **41**, 1101–1117.
73 R. Malacea, F. Chahdoura, M. Devillard, N. Saffon, M. Gómez, D. Bourissou, *Adv. Synth. Catal.*, 2013, **355**, 2274–2284.
74 R. Malacea, N. Saffon, M. Gómez, D. Bourissou, *Chem. Comm.*, 2011, **47**, 8163–8165.
75 B. E. Cowie, D. J. H. Emslie, *Chem. Eur. J.*, 2014, **20**, 16899–16912.
76 B. E. Cowie, D. J. H. Emslie, *Organometallics* 2013, **32**, 7297–7305.
77 B. E. Cowie, D. J. H. Emslie, *Organometallics* 2015, **34**, 4093–4101.
78 S. Bontemps, H. Gornitzka, G. Bouhadir, K. Miqueu, D. Bourissou, *Angew. Chem. Int. Ed.*, 2006, **45**, 1611–1614.
79 M. Sircoglou, S. Bontemps, M. Mercy, K. Miqueu, S. Ladeira, N. Saffon,L. Maron, G. Bouhadir, D. Bourissou, *Inorg. Chem.*, 2010, **49**(9), 3983–3990.
80 W. -C. Shih, W. Gu, M. C. MacInnis, S. D. Timpa, N. Bhuvanesh, J. Zhou, O. V. Ozerov, *J. Am. Chem. Soc.*, 2016 **138**, 2086–2089.
81 W. H. Harman, J. C. Peters, *J. Am. Chem. Soc.*, 2012, **134**, 5080–8082.
82 D. L. M. Suess, J. C. Peters, *J. Am. Chem. Soc.*, 2013, **135**, 12580–12583.
83 S. N. MacMillan, W. H. Harman, J. C. Peters, *Chem. Sci.*, 2014, **5**, 590–597.
84 W. H. Harman, T. –P. Lin, J. C. Peters, *Angew. Chem. Int. Ed.*, 2014, **53**, 1081–1086.
85 D. L. M. Suess, J. C. Peters, *J. Am. Chem. Soc.*, 2013, **135**, 4938–4941.
86 M. A. Nesbit, D. L. M. Suess, J. C. Peters, *Organometallics* 2015, 34(19), 4741–4752.
87 M. P. Boone, D. W. Stephan, *J. Am. Chem. Soc.*, 2013, **135**, 8508–8511.
88 A. Vigalok, B. Rybtchinski, Y. Gozin, T. S. Koblenz, Y. Ben-David, H. Rozenberg, D. Milstein, *J. Am. Chem. Soc.*, 2003, **125**, 15692–15693.
89 L. E. Doyle, W. E. Piers, J. Borau-Garcia, *J. Am. Chem. Soc.*, 2015, **137**, 2187–2190.
90 L. E. Doyle, W. E. Piers, J. Borau-Garcia, M. J. Sgro, D. M. Spasyuk, *Chem. Sci.*, 2016, **7**, 921–931.
91 B. W. H. Saes, D. G. A. Verhoeven, M. Lutz, R. J. M. Klein Gebbink, M.-E. Moret, *Organometallics* 2015, **34**, 2710–2713.
92 Q. Jing, C. A. Sandoval, Z. Wang, K. Ding, *Eur. J. Org. Chem.*, 2006, 3606–3616.
93 K. Ruhland, A. Obenhuber, S. D. Hoffman, *Organometallics* 2008, **27**, 3482–3495.
94 A. Obenhuber, K. Ruhland, *Organometallics* 2011, **30**, 4039–4051.
95 A. Obenhuber, K. Ruhland, *Organometallics* 2011, **30**, 171–186.
96 C.-S. Chen, C.-S. Lin, W.-Y. Yeh, *J. Organomet. Chem.*, 2011, **696**, 1474–1478.
97 W.-Y. Yeh, C.-S. Lin, *Organometallics* 2004, **23**, 917–920.
98 C. Tejel, M. A. Ciriano, M. Pilar del Rio, F. J. van den Bruele, D. G. H. Hetterscheid, N. Tsichlis i Spithas, B. de Bruin, *J. Am. Chem. Soc.*, 2008, **130**, 5844–5845.
99 W. I. Dzik, S. E. Calvo, J. N. H. Reek, M. Lutz, M. A. Ciriano, C. Tejel, D. G. H. Hetterscheid, B. de Bruin, *Organometallics* 2011, **30**, 372–374.
100 C. Tejel, L. Asensio, M. P. del Río, B. de Bruin, J. A. López, M. A. Ciriano, *Eur. J. Inorg. Chem.*, 2012, 512–519.
101 C. Tejel, L. Asensio, M. P. del Río, B. de Bruin, J. A. López, M. A. Ciriano, *Angew. Chem. Int. Ed.*, 2011, **50**, 8839–8843.
102 T. Büttner, F. Breher, H. Grützmacher, *Chem. Commun.*, 2004, 2820–2821.
103 P. Maire, A. Sreekanth, T. Büttner, J. Harmer, I. Gromov, H. Rüegger, F. Breher, A. Schweiger, H. Grützmacher, *Angew. Chem. Int. Ed.*, 2006, **45**, 3265–3269.

Dalton Transactions Accepted Manuscript

This journal is © The Royal Society of Chemistry 20xx

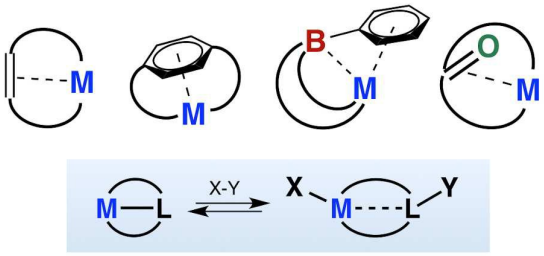

Recent advances in the use of tethered π-coordinating ligands for metal-ligand cooperation

Dalton Transactions Accepted Manuscript